



Strathprints Institutional Repository

Fleming, J.S. (2015) The energy efficiency of refrigerants : an assessment based on thermophysical properties. International Journal of Refrigeration, 58. pp. 235-242. ISSN 0140-7007 ,

This version is available at <http://strathprints.strath.ac.uk/54669/>

Strathprints is designed to allow users to access the research output of the University of Strathclyde. Unless otherwise explicitly stated on the manuscript, Copyright © and Moral Rights for the papers on this site are retained by the individual authors and/or other copyright owners. Please check the manuscript for details of any other licences that may have been applied. You may not engage in further distribution of the material for any profitmaking activities or any commercial gain. You may freely distribute both the url (<http://strathprints.strath.ac.uk/>) and the content of this paper for research or private study, educational, or not-for-profit purposes without prior permission or charge.

Any correspondence concerning this service should be sent to Strathprints administrator: strathprints@strath.ac.uk

**THE ENERGY EFFICIENCY OF REFRIGERANTS:
AN ASSESSMENT BASED ON THERMOPHYSICAL PROPERTIES**

J.S.Fleming

Honorary Research Fellow

Department of Mechanical and Aerospace Engineering

University of Strathclyde

Glasgow G1 1XJ, Scotland, UK

Corresponding author: J.S.Fleming, phone +441415638541, email j.s.fleming@strath.ac.uk

Abstract

A method is presented which ranks single fluid refrigerants in order of thermodynamic effectiveness. Blends can be included in the ranking if their viscosity is adjusted to account for blend constituent interactions. This is achieved by the empirical use of molecular acentricity and dipole moment values for the constituent fluids. Only public domain property data are needed.

Key Words

Refrigerants; thermal; effectiveness; ranking

1. Introduction

The man-made contribution to climate change is widely acknowledged. Refrigerant manufacturers have responded by developing new refrigerants which are lower in global warming effect when released into the environment – the direct effect. To maximise effectiveness this has to be combined with low energy consumption when the plant is running – the indirect effect.

The power consumed by a refrigerator or a heat pump is a function of the efficiency of the plant-refrigerant combination. This makes the contribution of the refrigerant on its own difficult to assess. This paper investigates the development of a method capable of giving a ranking order, best to worst, for the thermal effectiveness of refrigerants. It requires commonly available thermophysical properties only. Blends can be included in the assessment when an empirical adjustment is made to account for the dissipative interactions between blend components.

Nomenclature

Latin alphabet

C_1, C_2 etc	condensation factors
C_1, C_2	empirical constants
C_p, C_v	specific heat: constant press, vol (J Kg ⁻¹ K ⁻¹)
D	tube inner diameter (m)
E1, E2 etc	evaporation factors
f_i	constant in equation 4
g	acceleration of gravity (m s ⁻²)
G	mass flux (kg m ⁻² s ⁻¹)
h_{cond}	condensation heat transfer coefficient (W m ⁻² K ⁻¹)
h_{cc}	convective condensation heat transfer coefficient (W m ⁻² K ⁻¹)
h_{fc}	falling film condensation heat transfer coefficient (W m ⁻² K ⁻¹)
h_v	vapour heat transfer coefficient (W m ⁻² K ⁻¹)
h_{fg}	latent heat of vaporisation (kJ kg ⁻¹)
$I = C_p/C_v$	ratio of specific heats
$J_G = xG/[gD\rho_v(\rho_l - \rho_v)]^{0.5}$	dimensionless vapour velocity
k_l, k_v	conductivity: liquid, vapour (W m ⁻¹ K ⁻¹)
K_1	blend empirical constant
M	molecular weight
P	molecular polar moment (debye)
P, P_{red}	pressure, reduced pressure (Pa)
Pr_l, Pr_v	Prandtl number: liquid, vapour
q	heat flux (W m ⁻²)
$Re_{film} = [4G(1-x)\delta]/[(1-\alpha)\mu_l]$	Reynolds #: film
$Re_l = [G(1-x)D]/\mu_l$	Reynolds #: liquid
T_{sat}, T_{wall}	temperature: saturation, wall (deg C)
u_l, u_v	velocity: liquid, vapour (m s ⁻¹)
x	vapour quality
$X_{tt} = \left(\frac{\mu_l}{\mu_v}\right)^{0.1} \left(\frac{\rho_v}{\rho_l}\right)^{0.5} \left[\frac{(1-x)}{x}\right]^{0.9}$	= Martinelli parameter

Greek alphabet

α	void fraction
δ	film thickness (m)
$\mu_l, \mu_v, \bar{\mu}_l$	viscosity: liquid, gas, blend (Pa s)
π	circle: circumference/dia ratio
ρ_l	liquid density (kg m ⁻³)
ρ_v	gas density (kg m ⁻³)
σ	surface tension (N m ⁻¹)
ω	molecular acentricity (-)

Subscripts

$cond$	condensation
cc	convective condensation
fc	falling film condensation
v	vapour
l	liquid

2. The basis of the method

The ASHRAE Fundamentals Handbook of 2001 (2001) explains the methodology by which its coefficient of performance (cop) values are determined for refrigerants. In the method presented here a cycle factor is determined for each refrigerant which is a function of fluid properties alone. The cycle factors are compared with the cop values and the trend examined. Where it gives the same order for the factors as for the cop values this is taken to be a strong indication that the method has value in ranking refrigerants in order of thermal effectiveness.

3. Refrigeration and heat pump applications

The essential features of refrigerators and heat pumps are identical as represented in diagrammatic form in figure 1.

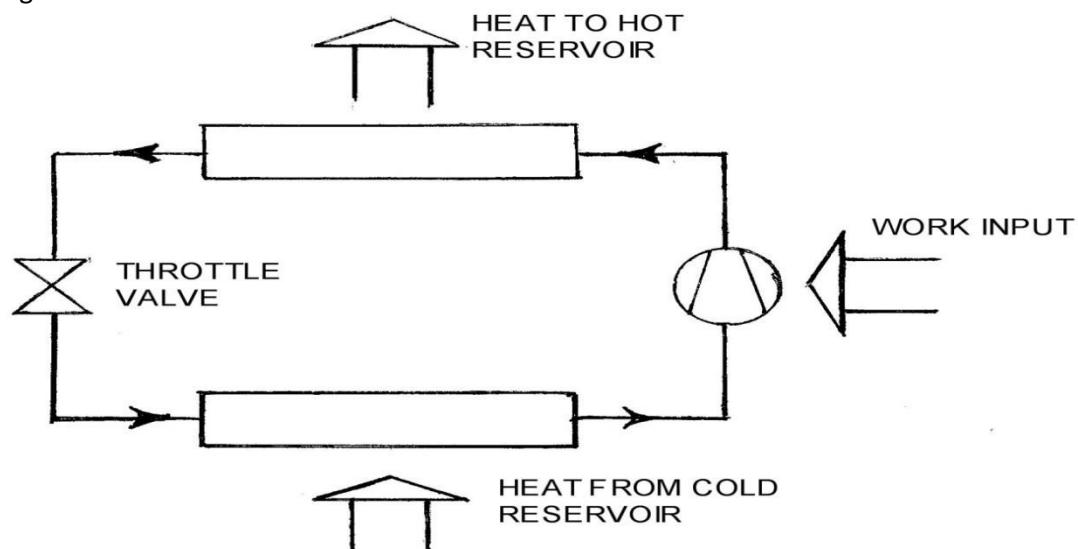


Figure 1 Basic circuit of heat pump and refrigeration systems

4. The cycle factor method

Interest has grown in the use of natural substances such as carbon dioxide, ammonia, hydrocarbons, and air as refrigerants. In addition, new less polluting synthetic refrigerants have been introduced. Heat transfer, already a heavily researched area, received increased effort, especially that occurring during evaporation and condensation, the most common methods in use for drawing heat from the cold reservoir and releasing heat to the hot reservoir, respectively.

The cycle factor used here is a function of three factors: one for the evaporator, one for the compressor and one for the condenser. The ratio of the specific heats is used as the compression factor. The evaporation and condensation factors are derived from two sources:

- heat transfer expressions from the literature,
- a qualitative consideration of the behaviour of refrigerants during phase change.

5. Published work on heat transfer during phase change

5.1 General comments

More work has been published on phase change in a fluid flowing in a horizontal tube than in any other arrangement. The heat transfer calculations for this case are complex due to the combined influence of: fluid properties, the liquid/gas ratio which changes along the tube length and the flow regime which is a function mass flux, heat flux, pressure and temperature. Each flow regime requires a different equation for the calculation of heat transfer. Measured data is used to derive the criteria which define flow regime and the associated expressions for heat transfer.

5.2 Literature

5.2.1 Condensation

Cavallini et al. (2001, 2006) summarised their own work and the work of others on flow condensation heat transfer characteristics and proposed correlations for various refrigerants. They used two dimensionless parameters to identify flow regime, a dimensionless vapour velocity J_G and the Martinelli parameter (2002). Thome et al. (2003) determined flow regime from a 'map' based on a flow pattern map proposed by Kattan et al. (1998). Both Cavallini et al. (2002) and Thome et al. (2003) proposed that two condensation mechanisms provide the main contribution to in-tube flow condensation:

- Convective condensation influenced by vapour shear and turbulence which results in an axially flowing liquid film on the tube wall.
- Falling film condensation in the liquid film which falls under the influence of gravity down the upper part of the tube wall.

Flow pattern prediction is critical to success of heat transfer calculations because the equation appropriate to the flow pattern must be used. For example falling film condensation can only exist when a stratified flow pattern exists. In an attempt to improve the predictive capacity of the equations of Cavallini et al. (2002) and Thome et al. (2003) for ammonia, Hrnjak and Park (2007) made use of measured data provided by Komandiwirya et al. The flow pattern recognition system determines the dry radial angle (θ) for the tube surface which is used as shown in equation (1). The flow condensation heat transfer coefficient can be expressed as follows:

$$h_{cond} = h_{cc} \left(\frac{2\pi - \theta}{2\pi} \right) + h_{fc} \left(\frac{\theta}{2\pi} \right) \quad (1)$$

$$h_{cc} = C_1 Re_{film}^{C_2} Pr_l^{0.3} \left(\frac{k_l}{\delta} f_i \right) \quad (2)$$

$$h_{fc} = C_3 \left[\frac{g \rho_l (\rho_l - \rho_v) h_{fg} k_l^3}{\mu_l D (T_{sat} - T_w)} \right]^{0.25} \quad (3)$$

$$f_i = 1 + \left(\frac{u_v}{u_l} \right)^{0.5} \left(\frac{g (\rho_l - \rho_v) \delta^2}{\sigma} \right)^{0.25} \quad (4)$$

5.2.2 Evaporation

The equations of Zurcher et al. (1999) for calculating heat transfer in flow evaporation for ammonia are given below. Similar algebraic forms are in use for other fluids. Flow pattern recognition is needed.

$$h_{evap} = (h_{nb}^3 + h_{cb}^3)^{\frac{1}{3}} \left(\frac{2\pi - \theta_{dry}}{2\pi} \right) + h_v \left(\frac{\theta_{dry}}{2\pi} \right) \quad (5)$$

$$h_{nb} = 55 P_{red}^{0.12} (-\log_{10} P_{red})^{-0.55} M^{-0.5} q^{0.67} \quad (6)$$

$$h_{cb} = 0.0133 \left[\frac{5G(1-x)\delta}{(1-\alpha)} \right]^{0.69} Pr_l^{0.4} \frac{k_l}{\delta} \quad (7)$$

$$h_v = 0.023 \left(\frac{GxD}{\alpha\mu_v} \right)^{0.8} Pr_v^{0.4} \frac{k_v}{D} \quad (8)$$

The flow pattern map of Zurcher et al. (1999) is shown in figure 2.

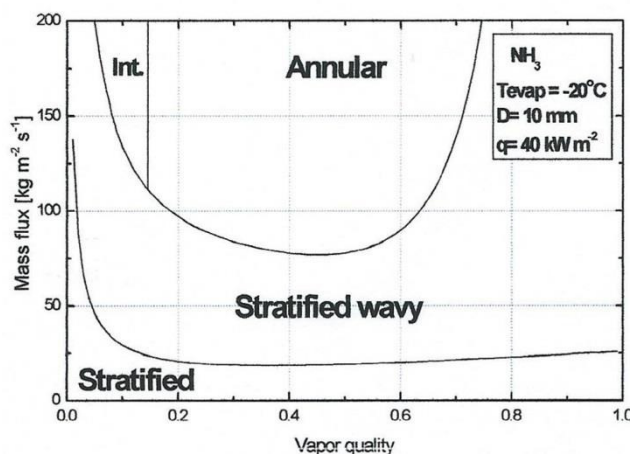


Figure 2 Flow pattern map for NH₃

6. A qualitative consideration of fluid behaviour

6.1 Condensation

It is clear from equations (1), (2), (3) and (4) that liquid fluid properties dominate. This is in accord with observed behaviour in which the formation of the liquid film on the tube wall and its travel along and down the wall under the influence of fluid shear and gravity are the principal physical influences. This guides the weighting of the properties in the trial condensation factors in the process of matching the cycle factor sequence with the cop sequence.

6.2 Evaporation

It is not obvious from equations (5), (6), (7) and (8) which is more important, liquid or gas behaviour. A detailed examination of evaporation in flow boiling is now given with a view to revealing the dominant influences. This informs the weighting of properties in the evaporation factor in the process of matching the cycle factor sequence with the cop sequence.

Yun et al. (2003) conducted an experimental study in which the evaporative heat transfer performance of carbon dioxide was compared with that of R134a a synthetic refrigerant. The difference between these two fluids is very clear. This makes a detailed discussion of their evaporative behaviour particularly revealing when considering the influence of fluid properties. The thinking needed provides a guide to deriving simple factors for evaporation.

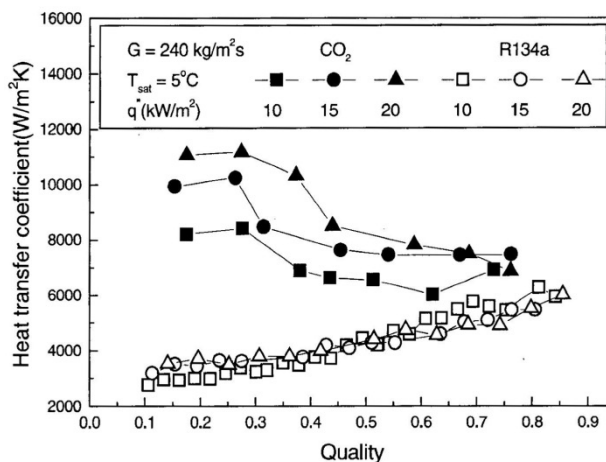


Figure 3 Evaporative heat transfer coefficients for CO2 and R134

The exceptional heat transfer performance of R744 seen in figure3 is due to its unusual properties which differ greatly from those of R134a and similar refrigerants. As the R744 passes from the low quality region near the entrance of the evaporator where it is mostly liquid, to the high quality region near the exit where it is mostly gas, several changes of flow regime occur. However, only two mechanisms of heat transfer are significant - nucleate boiling and convection. Nucleate boiling, more effective as a heat transfer mechanism than convection at these saturation temperatures, can only occur in the liquid present and since there is around ten times more liquid present per unit volume at any chosen quality when the refrigerant is R744, a huge advantage is gained over R134a in heat transfer. The abundance of liquid is due to the specific volume ratio, liquid to gas, which for R744 is approximately ten times greater than that of R134a at 5°C.

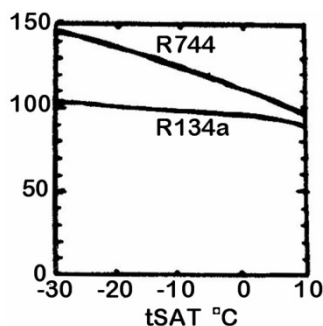


Figure 4 Liquid conductivity $mW (mK) - 1$

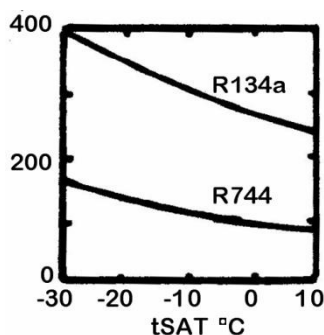


Figure 5 Liquid viscosity $\mu Pa.s$

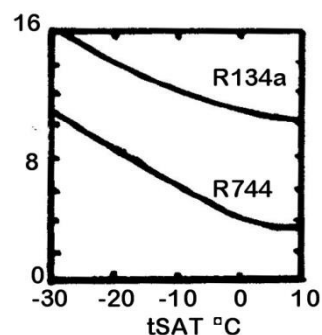


Figure 6 Surface tension $mN m - 1$

Conductivity, viscosity and surface tension for liquid R744 and R134a are compared in figures 4, 5 and 6. Heat transfer is enhanced by high conductivity in combination with low viscosity. R744 has a clear advantage over R134a. However, flow boiling is not a simple process. Surface tension is lower and the saturation pressure much higher for R744. The influence of this combination is not obvious.

Lock (1996) discusses bubble growth at nucleation sites, bubble size at detachment, and bubble growth/shrinkage as a bubble moves buoyantly upwards through the liquid refrigerant. His equations indicate that R744 bubbles at release from their nucleation sites are smaller than those of R134a, which leaves more room on the heated surface for the birth of new R744 bubbles. Also, R744 bubbles are released from the tube surface earlier than those of R134a.

Furthermore, his equations indicate that the bubble growth/shrinkage rate for R744 is twice that of R134a during buoyancy-driven migration through the liquid refrigerant. As a consequence, R744 bubbles perform their heat transfer/transport function at a higher rate than those of R134a, which is in accord with the behaviour seen in figure 3.

Bubbles which collapse into the liquid before reaching the surface, transfer the heat of their gas to the parent fluid. Those which survive to reach the surface, burst in a disorderly manner. This projects liquid droplets into the gas flowing above the liquid, an effect which is greater for R744 than for R134a. These droplets move with the gas, but can also migrate within it due to turbulence and convection, which enhances convective evaporation as dry-out progresses due to the larger number of smaller-sized droplets in the R744 droplet population.

The disorderly nature of the flow of the liquid along the tube results in wetting and run-off from the upper areas of the tube inner surface. The low surface tension and viscosity of liquid carbon dioxide causes it to have a higher propensity to run off the upper part of the tube inner surface than is the case with liquid R134a. The net effect on evaporation will depend on local heat and mass flows which are difficult to estimate, which makes predictions very uncertain. Clearly, relying on a discussion of property characteristics alone to predict refrigerant behaviour is inadequate. Measured data or property values used in accordance with the mechanics of thermofluids are needed.

Figures 7 and 8 show that gas density and conductivity are also significantly higher for R744 than for R134a at all saturation temperatures of interest. Measurements like those shown in figure 3 are needed to demonstrate that the higher gas viscosity (figure 9) is not a significant disadvantage.

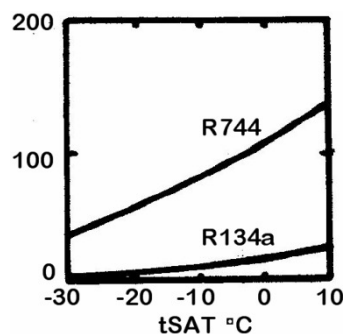


Figure 7 Gas density $kg\ m^{-3}$

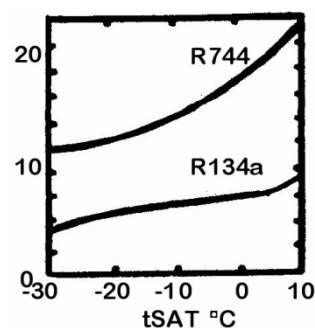


Figure 8 Gas conductivity $mW\ (m\ K)^{-1}$

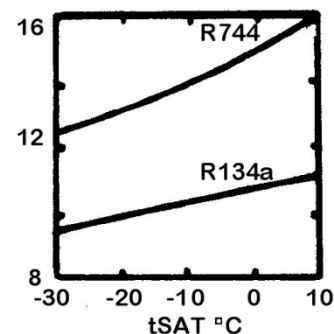


Figure 9 Gas viscosity $\mu Pa\ s$

The above considerations improve knowledge of refrigerant behaviour and can assist with the detail design of heat exchanges but do not lead to a practical numerical method by which refrigerants can be ranked. They guide choice in determining the order of importance of properties.

7. Property-dependent factors for cycle components

The production of measured heat transfer coefficients like those shown in figure 3 is resource-intensive, time-consuming and hence expensive. Pearson (2005) discusses in some detail the manner in which fluid properties influence heat transfer and pressure drop in refrigeration plant. He also makes use of a cop ranking order given in the ASHRAE literature (2001). The same data was used here in a pilot study in the development of the cycle factor method.

Hrnjak and Park (2007) showed that equations of the same general form can be used to calculate evaporative heat transfer for ammonia and carbon dioxide, two very different refrigerants. They also show that similar equations from the literature, which is vast, can be used for other refrigerants providing that the empirical constants are appropriate.

The first choices for evaporation and condensation factors (equations (9) and (11)) were inspired by the expressions for heat transfer coefficients given in equations (1) to (8). The qualitative treatment of phase change behaviour described in 6.1 and 6.2 was then used to inform the choice of trial variants of the factors. The ratio of the specific heats at the average temperature was chosen as the compression factor. The three factors were used to calculate a cycle factor for the complete basic cycle (figure 1). The ranking of the refrigerants best to poorest is compared with the ASHRAE ranking for cop (2001), for the same temperatures (the U.S. standard cycle, evaporation -15°C , condensation 30°C).

The first choices for the factors were as follows.

$$\text{Evaporation factor} = \left[\frac{\mu C_p}{k} \right]_{liq}^{0.4} k_l = E \quad (9)$$

$$\text{Gas compression factor} = \frac{C_p}{C_v} = \text{isentropic index} = I \quad (10)$$

$$\text{Condensation factor} = \left[\frac{\rho_l(\rho_l - \rho_v)}{\sigma \mu_l} k_l^3 h_{fg} \right]^{1/4} = C \quad (11)$$

$$\text{Cycle factor} = \frac{E * C}{I} \quad (12)$$

The pilot trial sequence is shown below.

TABLE 1 Trial Cycle Factors

Trial E factors, evaporation at -15 C	R717	R290	R600	R22	R134a	R407C	R410A	R404A
$E1 = \left[\frac{\mu_l C_p}{k_l} \right]^{0.4} k_l$	715.2	179.6	220.4	154.6	177.8	178.0	173.6	137.2
$E2 = \left[\frac{\mu_l C_p}{k_l} \right]^{0.4} k_l \frac{\sigma}{\mu_l}$	134.2	14.58	15.6	8.42	7.43	9.18	9.61	5.92
Index of compression at 7.5 C								
I	1.415	1.23	1.122	1.311	1.191	1.302	1.414	1.272
Trial C factors, condensation at 30 C								
$C1 = \left[\frac{\rho_l(\rho_l - \rho_v)}{\sigma \mu_l} k_l^3 h_{fg} \right]^{1/4}$	1947	625	526	574	539.3	625.7	759	526.6
$C2 = \left[\frac{\rho_l(\rho_l - \rho_v)}{\sigma \mu_l} k_l^3 h_{fg} \right]^{1/4} \frac{\sigma}{\mu_l}$	361.4	43.3	38.9	27.04	21.57	26.6	28.77	17.41
$C3 = \left[\frac{\rho_l(\rho_l - \rho_v)}{\sigma \mu_l} k_l h_{fg} \right]^{1/4}$	89.7	65.37	51.34	63.63	60.68	66.58	77.14	65.31
$C4 = \left[\frac{\rho_l(\rho_l - \rho_v)}{\sigma \mu_l} k_l h_{fg} \right]^{1/4} \frac{\sigma}{\mu_l}$	16.65	4.524	3.80	3.00	2.43	2.83	2.925	2.16
Trial cycle factors								
$E1 * C1/I$	973092	91707	103040	66472	79512	85871	88908	55068
$E2 * C2/I$	33892	515.2	539.8	170.5	132.9	188.3	186.6	78.6
$E2 * C4/I$	1561	53.89	52.69	18.92	14.97	20.04	18.97	9.25
ASHRAE COP	4.84	4.74	4.68	4.65	4.60	4.51	4.41	4.21

8. Discussion

8.1 Pilot study: US standard cycle

The cycle factor sequence given in the third trial is in accord with that given for COP by ASHRAE (2001) for all but two of the refrigerants, both of which are blends, R407C and R410A. R404A is also a blend with a small glide but is predicted to be in its correct ASHRAE location in the sequence, last. The single fluids, R717, R290, R600, R22, and R134a, are in the same sequence as the ASHRAE cop sequence.

The disorderly nature of the flow in the evaporator and the condenser, combined as it is with phase change could be accompanied by additional irreversibilities for the blends, due to interactions between the blend components. The influence of the physics of the associative effects of blend mixing is not expressed numerically in Table 1 and hence is not taken into account. According to Reid (1987) even mild association effects between components can significantly affect the viscosity of the mixture. The system presented here places blends R407C and R410A three positions higher than in the cop sequence. Reid (1987) states that the tabulated property values given for blends are calculated by interpolation of the constituent values but many methods are available and the compilers of the tables rarely give detail of the method used.

Thermodynamic irreversibility is more sensitive to viscosity than to any other basic property. Hence an increase in viscosity will result in a reduction in thermodynamic effectiveness. The viscosity of a blend is sensitive to the molecular characteristics of the blend constituents. **Acentricity** is a numerical measure of the departure of the molecular geometry from sphericity. **Dipole moment** is also related to the geometry of the molecule and to unbalanced electrostatic charges on the outer electron shell. Values are given by Weast (1984). The cause of unbalanced charge can be seen by examining two simple molecules, those of carbon dioxide and water as shown in figure 10.

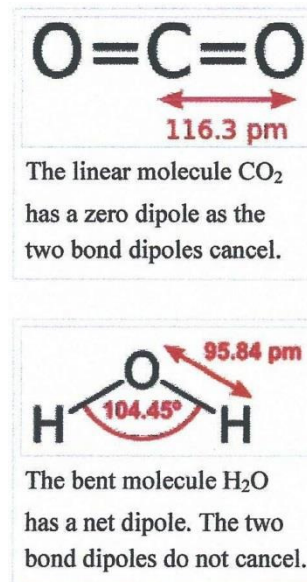


Figure 10 Zero and non-zero dipole moments

The values for acentricity ω and dipole moment P for the blend constituents are shown in Table 2. The ratio of dipole moment to acentricity gives a numerical value related to the electrostatic charge on the outer electron shell. This value was used in the empirical expression (equation 13) to calculate a blend viscosity higher than that given in the ASHRAE tables. The P/ω values for the blends were calculated by adding the contributions of the blend constituents according to their mass fractions.

TABLE 2 Dipole moments, acentricities and their ratios

	Unit	R134a	R32	R125	R143a		R407c	R410a	R404a
ω	-	0.326	0.278	0.305	0.259		-	-	-
P	debye	2.06	2.27	1.56	2.33		-	-	-
P/ω	debye	6.319	8.165	5.115	8.996		6.443	6.640	7.180

Blend composition

R407c R32/R125/R134a 23/25/52

R410a R32/R125 50/50

R404a R125/R143a/R134a 44/52/4

The empirical constant K_1 in equation (13) was chosen to give a cycle factor a value for R407C a little smaller in value than that of R134a. The R410a and R404a cycle factors were then re-calculated using equation 13 to determine viscosity. This placed the blend cycle factors in the sequence shown in Table 3. It is the same as that given by ASHRAE for cop (2001).

$$\bar{\mu} = K_1 \frac{P}{\omega} \mu \quad (K_1 = 0.1958) \quad (13)$$

TABLE 3 New cycle factor sequence

	R717	R290	R600	R22	R134a	R407C	R410A	R404A
New cycle Factor	1561	53.89	52.69	18.92	14.97	13.72	12.35	5.49
ASHRAE COP	4.84	4.74	4.68	4.65	4.60	4.51	4.41	4.21

8.2 Different refrigerants at different operating conditions

To test the method with different refrigerants and temperatures the ASHRAE Fundamentals Handbook for 2013 (2013) was consulted. Only one new refrigerant became available, R1234yf. The condensing temperature was the same in all cases, 30°C. Two new evaporating temperatures became available, -6.7°C and 7.2°C. The cycle factor trend is shown in figures 11, 12 and 13. Cycle factors for R717 and R290 are part of the data set and are in their 'correct' sequence but have cycle factors which are too high to appear in the figures.

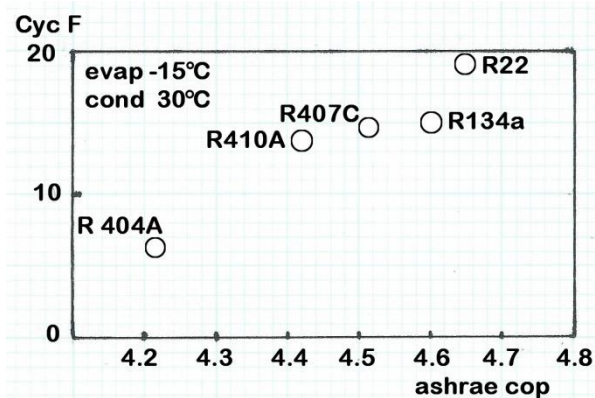


Figure 11 Evaporating temperature -15°C

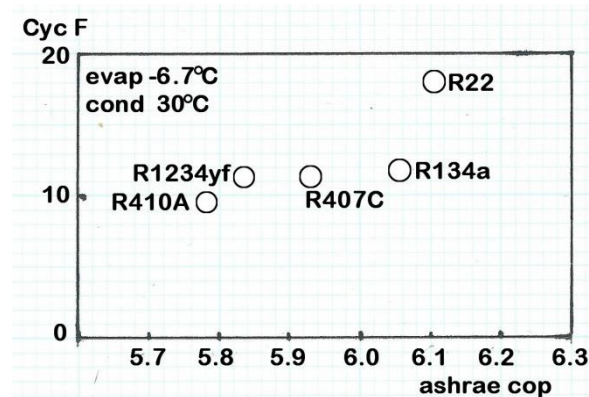


Figure 12 Evaporating temperature -6.7°C

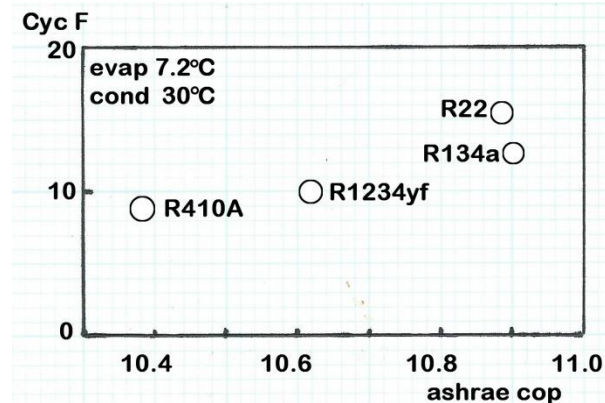


Figure 13 Evaporating temperature 7.2°C

9. Concluding comments

The great majority of the refrigerants in use have critical temperatures in the region 80°C to 130°C. This investigation was confined to refrigerants with critical temperatures in this range. The factor method places R134a one place high in the sequence when the evaporating temperature is 7.2°C and R290 two places high for evaporating temperatures -6.7 °C and 7.2 °C.

The factor method provides a guide to ranking refrigerants, based solely on their properties, in their order of thermal effectiveness.

Before use is made of the viscosity values given for blends by ASHRAE (2001, 2013) consideration should be given to the possible influence of blend association effects.

References

ASHRAE, 2001. *Fundamentals Handbook*.

ASHRAE, 2013. *Fundamentals Handbook*.

Cavallini, A., Censi, G., Del Col, D., Doretti, L., Longo, G. A., Rossetto, L., Zilio, C. 2001 Experimental investigation on condensation heat transfer and pressure drop. *Int. J. Refrigeration*. 24, 1, 73 – 87.

Cavallini, A., Censi, G., Del Col, D., Doretti, L., Longo, G. A., Rossetto, L., Zilio, C. 2002. In-tube condensation of halogenated refrigerants. *ASHRAE Trans*, 108, 146 – 161.

Cavallini, A., Censi, G., Del Col, D., Doretti, L., Longo, G. A., Rossetto, L., Zilio, C. 2006. Condensation inside and outside smooth and enhanced tubes – a review of recent research. *Int. J. Refrigeration* 29, 7, 1100 – 1108.

Hrnjak, P.S., Park, C.Y. 2007. In-tube heat transfer and pressure drop characteristics of pure NH₃ and CO₂ in refrigeration systems. *IIR Conference: ammonia refrigeration technology for today and tomorrow*, Ohrid.

Kattan, N., Thome, J.R., Favrat, D. 1998. Flow boiling in horizontal tubes: part 1 Development of a diabatic two-phase flow pattern map. *J Heat Transfer*, 120, 140 – 147.

Komandiwirya, H.B., Hrnjak, P.S., Newell, T.A. An experimental investigation of pressure drop and heat transfer in an in-tube condensation system of ammonia with and without miscible oil in smooth and enhanced tubes. *ACRC CR – 54*, University of Illinois at Urbana- Champaign

Lock, G. S. H. 1996. Latent Heat Transfer. *Oxford University Press*, U.K.

Pearson, A.B., 2005. The optimisation of carbon dioxide refrigeration systems. *University of Strathclyde PhD thesis*.

Reid, R. C., Prausnitz, J. M., Poling, B. E. 1987. The Properties of Gases and Liquids *McGraw-Hill, New York*.

Thome, J.R., El Hajal, J., Cavallini, A. 2003. Condensation in horizontal tubes, part 2: a new heat transfer model based on flow regimes *Int. J. Heat and Mass Transfer*, 46, 18, 3365 – 3387.

Weast, R.C. 1984 CRC Handbook of Chemistry and Physics (65th Ed.). CRC Pres

Yun, R., Kim, Y., Kim, M. S., Choi, Y. 2003. Boiling heat transfer and dry-out phenomena of CO₂ in a horizontal smooth tube. *Int. J. Heat and Mass Transfer*. 46, 2253 – 2361

Zurcher, O., Thome, J.R., Favrat, D. 1999. Evaporation of ammonia in a smooth horizontal tube: heat transfer measurements and predictions. *J. Heat Transfer*, 121, 89 – 101.